Anesthesiology 2005; 103:1218–24 

# *Frontal Slab Composite Magnetic Resonance Neurography of the Brachial Plexus*

## *Implications for Infraclavicular Block Approaches*

*David T. Raphael, M.D., Ph.D.,* Diane McIntee, M.S.,† Jay S. Tsuruda, M.D.,‡ Patrick Colletti, M.D.,§ Ray Tatevossian, M.D.‖*

***Background:*** **Magnetic resonance neurography (MRN) is an imaging method by which nerves can be selectively highlighted. Using commercial software, the authors explored a variety of approaches to develop a three-dimensional volume-rendered MRN image of the entire brachial plexus and used it to evaluate the accuracy of infraclavicular block approaches.**

***Methods:*** **With institutional review board approval, MRN of the brachial plexus was performed in 10 volunteer subjects. MRN imaging was performed on a GE 1.5-tesla magnetic resonance scanner (General Electric Healthcare Technologies, Waukesha, WI) using a phased array torso coil. Coronal STIR and T1 oblique sagittal sequences of the brachial plexus were obtained. Multiple software programs were explored for enhanced display and manipulation of the composite magnetic resonance images. The authors developed a frontal slab composite approach that allows single-frame reconstruction of a three-dimensional volume-rendered image of the entire brachial plexus. Automatic segmentation was supplemented by manual segmentation in nearly all cases. For each of three infraclavicular approaches (posteriorly directed needle below midclavicle, infracoracoid, or caudomedial to coracoid), the targeting error was measured as the distance from the MRN plexus midpoint to the approach-targeted site.**

***Results:*** **Composite frontal slabs (coronal views), which are single-frame three-dimensional volume renderings from image-enhanced two-dimensional frontal view projections of the underlying coronal slices, were created. The targeting errors (mean ± SD) for the approaches—midclavicle, infracoracoid, caudomedial to coracoid—were 0.43 ± 0.67, 0.99 ± 1.22, and 0.65 ± 1.14 cm, respectively.**

***Conclusion:*** **Image-processed three-dimensional volume-rendered MNR scans, which allow visualization of the entire brachial plexus within a single composite image, have educational value in illustrating the complexity and individual variation of the plexus. Suggestions for improved guidance during infraclavicular block procedures are presented.**

MAGNETIC resonance neurography (MRN) is an imaging modality that can reliably and selectively image peripheral nerves.[1,2] In MRN, the use of pulsed magnetic gradients, oriented parallel and perpendicular to the nerve orientation, exploits the difference in T1 and T2 relaxation differences and/or diffusional anisotropy of peripheral nerve tissue *versus* muscle and enhances the intensity of the nerve signal relative to the surrounding tissue.

A peripheral nerve has loose fatty connective tissue between and around its fascicles. The nerve fibers are surrounded by a compact layer of collagenous perineurium. The axons, Schwann cells, and endoneurium are bundled together into fascicles, each of which is encompassed by a collagenous perineurium. An outer connective tissue sheath, the epineurium, envelops the nerve and the fascicles. Fascicles in cross-sectional views appear in high-tesla MRN as dot-like honeycomb structures.[3] Magnetic resonance (MR) imaging difficulties arise because the longitudinal course of the plexus at varying depths from the skin surface leads to variable signal-to-noise (SNR), which leads to bulk susceptibility artifact and inhomogeneity of fat saturation.

To improve image contrast in nerve imaging, the interfascicular fat signal must be suppressed. This can be accomplished with long TR sequences (T2-weighted fast spin echo with fat suppression) and *via* fat-suppressive STIR sequences.[2,3] In a STIR sequence (short T1 inversion recovery), fat suppression is attainable at all field strengths due to the short T1 relaxation properties of lipids. In this sequence, the longitudinal magnetization is first inverted by a 180° pulse, which causes all tissues to have negative values. The longitudinal magnetization of fat becomes progressively less negative at a faster rate than other tissues. Because fat has the shortest T1 (250–350 ms) of most substances in the body, it passes through its null point (the point of zero magnetization) first before other tissues do. At the null point, fat suppression is effected, while the remaining tissues still have a negative longitudinal magnetization. These negative values are then inverted and appear bright in the final image in direct proportion to their T1 values.[4] This technique allows the creation of an MRN image, where the peripheral nerve tract remains the most prominent feature in the generated image. This has allowed MRN selective imaging of the brachial plexus for diagnostic purposes to become an established radiologic procedure.[5–7]

Our goal in this study was to develop a method by which to transform the sequence of discontinuous two-dimensional (2-D) MRN images, each of which exhibits a

* Associate Professor, Director of Anesthesia Research, † Special Projects Manager, ‖ Resident, Department of Anesthesiology, § Professor of Radiology, Keck School of Medicine, University of Southern California. ‡ Chief Scientific Officer, The Neurography Institute, Santa Monica, California. Visiting Scholar, Department of Radiology, University of Utah School of Medicine, Salt Lake City, Utah.

Received from the Department of Anesthesiology, Keck School of Medicine, University of Southern California, Los Angeles, California. Submitted for publication March 10, 2005. Accepted for publication July 7, 2005. Supported by the Foundation for Anesthesia Education and Research, Rochester, Minnesota. Cosponsor: AstraZeneca Pharmaceuticals, Wilmington, Delaware. Presented as a poster at the International Anesthesia Research Society Meeting, Honolulu, Hawaii, March 11–15, 2005, and as an oral presentation at the Western Anesthesia Residents Meeting, Irvine, California, April 30–May 1, 2005.

Address reprint requests to Dr. Raphael: Department of Anesthesiology, Keck School of Medicine, University of Southern California, 1200 North State Street, Room 14-901, Los Angeles, California 90033. Address electronic mail to: draphael@usc.edu. 

component segment of the brachial plexus, into a single-frame composite three-dimensional (3-D) volume-rendered MRN image of the entirety of the plexus. For multiple subjects, we then used the composite 3-D MRN volume-rendered image as a method by which to determine the accuracy of needle placement recommendations for three infraclavicular regional block approaches.

## Materials and Methods

With approval of the institutional review board (University of Southern California, Los Angeles, California) and written informed consent, MRN of the right brachial plexus was performed in 10 adult volunteer subjects in the supine position, with arms adducted and head slightly rotated to the left. Subjects (3 men, 7 women) were aged (mean ± SD) 47 ± 10 yr, weighed 69 ± 11 kg, and were 167.5 ± 9.6 cm tall. All studies were performed on a GE 1.5-tesla MR scanner (General Electric Healthcare Technologies, Waukesha, WI) with 9.0 software and HighSpeed gradient platform using a four-channel phased array torso coil.

*Scanning Techniques*

Coronal and oblique sagittal STIR sequences of the brachial plexus were obtained using 4- to 6-mm slices (no interslice gap) as follows:

1. Coronal STIR sequence parameters: TR 4,500 ms, effective TE 40 ms, TI 150 ms. Echo train length 16 with 4 excitations. Resolution parameters: field of view 22 cm, slice thickness 4 mm, skip 0 mm (no interslice gap), 256 frequency and 224 phase encoding steps. Frequency direction and flow compensation was directed in the superior–inferior direction.
2. Oblique sagittal STIR with slice orientation perpendicular to the long axis of the brachial plexus: TR 4,500 ms, effective TE 40 ms, TI 150 ms. Echo train length 16 with 4 excitations. Resolution parameters: field of view 14 cm, 4- to 5-mm slices, skip 0 (no interslice gap), 256 frequency and 192 phase encoding steps. Frequency gradient was oriented in the superior–inferior direction with flow compensation in the slice direction.
3. Oblique sagittal T1 sequence parameters: TR 600 ms, effective TE 12 ms. Echo train length 4 with 3 excitations. Resolution parameters: field of view 14 cm, 4- to 5-mm slices, skip 0 (no interslice gap), 256 frequency and 192 phase encoding steps. Frequency direction was directed anteroposteriorly with flow compensation in the slice direction.

The proximity of arteries, veins, and the lungs results in significant breathing and flow artifacts that must be minimized. Measures taken to reduce artifacts included the use of "presaturation" pulses, applied before a radiofrequency excitation pulse; the use of saturation bands, which helps to suppress blood flow artifacts and movement ghosts; flow compensation, to saturate inflowing blood; and use of a selective phase direction, to lessen motion and flow artifacts carried through the images in the phase direction. It should be noted that flow compensation pulses and saturation bands do not entirely remove artifact from flowing blood.

*Image Processing*

Multiple software programs were explored for possible display and manipulation of the MR images. The brachial plexus component of each composite slab was created from an average of 10 (range, 5–12) sequential coronal slices from an original total of 20 slices. The slices were selected by viewing the entire data set in the DicomWorks viewer program, version 1.3.5.# DICOM is short for Digital Imaging and Communications in Medicine and is a standard in the field of medical informatics for exchanging digital information between medical imaging equipment (such as radiologic imaging) and other systems. Image processing programs used were PhotoShop version 7.0 and ImageReady version 7.0 (Adobe Systems Inc., San Jose, CA). Automatic segmentation, which depends on distinguishing different gray levels, was inadequate to separate the subtle differences of the nerves from the surrounding tissue and required supplemental manual segmentation, complete or partial, in nearly all cases.

We developed a composite frontal slab approach, which consists of enhanced 2-D frontal view projections of a limited number of coronal slices onto a single composite 3-D volume-rendered slice. The selected 2-D slices were those that included a brachial plexus component, whereas all non–plexus-related slices were excluded, other than those required to complete the background skeletal composite. Had we excluded all images lacking a brachial plexus component, we might have excluded images of bony structures relevant to nerve blocks and made it more difficult for the viewer to appreciate the block-related plexus anatomy. Hence, a minimal number of slices were added to the composite that would provide a reference skeleton, both in terms of background (spine) and foreground (clavicle, coracoid, humerus). To enhance slab image realism, the background image was created by merging two nonconsecutive representative slices from the data set that would reflect the directional course of the right-sided brachial plexus, *i.e.*, from the upper medial to the lower lateral. Hence, a background image at the medial cephalad region, at the level of the vertebral spine, was interconnected with a more shallow background image, which reflected the more anterior and lateral portion of the brachial plexus.

These images are not free of conventional MR imaging

# DICOM Works. Available at: http://dicom.online.fr. Accessed September 8, 2005.

difficulties. A "partial voluming" structure discontinuity can be produced with the thicker 2-D slices (4–6 mm), when the studied structure (*e.g.*, thin nerve in the axilla) is comparable in size to the voxel (a voxel is defined as a pixel times slice thickness). When the structure straddles two adjacent voxels, it may not be possible to separate the signals from different tissue compartments, and this can result in imperfect continuity and diminished brightness in the resulting image. However, there has been no insertion of any extraneous images to patch up seeming discontinuities, as might occur at nerve branch points.

The frontal slab composite–MRN image segmentation approach shares a common "projection" aspect with the maximum intensity projection technique used in angiography. Maximum intensity projection is an automated technique, commonly used in angiography, where the brightest voxel in a 2-D slice (usually that corresponding to the vessel) is projected onto a composite image. Unlike this automated technique, frontal slab composite–MRN involves a qualitative identification of the nerve component (independent of the maximal brightness) and a segmentation of the nerve image, which is then projected onto a composite image.

Each of the identified slices was converted into a TIFF file in DICOM Works. These TIF files were then brought in as sequential layers in the form of a single Adobe Photoshop image, while maintaining the original order of slices. For improved spatial resolution and edge detection, the image display matrix was increased from $256 \times 256$ pixels to $1{,}024 \times 1{,}024$ pixels using Photoshop's bicubic resampling method.

Using the selection and mask tools in Photoshop, the areas of interest (bones, nerves, vessels) were cropped appropriately on each layer of the Photoshop image. Blending between the layers was done to create smooth transitions. The structures of interest were enhanced (using the dodge and burn tool) or colorized with semitransparent color to bring out the details and emphasize the structures that were atop underlying ones. Specifically, bony structures used as reference landmarks (coracoid process, clavicle) were colorized. The areas of interest (nerve, vessels, bone) were manually segmented using Photoshop's selection tools and filled with different semitransparent colors. The transparency of the color was typically set to 30% opacity— enough to tint the area with color but still allow the underlying structures to show through. Each of these colorized slices in the data set was brought in as a sequential layer in one composite Photoshop image (keeping the original order of slices).

*Brachial Plexus Needle Targeting*

For each subject, a composite 3-D volume-rendered MRN image of the brachial plexus was obtained. Using the composite MRN plexus as the reference structure, we assumed that ideal needle placement, for any infraclavicular approach that relies on a posteriorly directed needle, was for the needle to be directed toward the plexus midpoint (defined as the midpoint of the MRN plexus along its vertical extent). We compared three anatomical landmark–based infraclavicular approaches that rely on a posteriorly directed needle and determined their targeting accuracy relative to the frontal midplexus location specified by the composite MRN image. Specifically, we examined two coracoid approaches[8,9] (2 cm medial and 2 cm caudad to coracoid, or 2–3 cm caudad to coracoid) and one midclavicular[10] (using a needle directed posteriorly immediately below the midclavicle) and ascertained the specific point in the plexus targeted by a posteriorly directed needle. Hence, the targeting error (mean $\pm$ SD) for any one approach was measured as the distance from the true MRN midplexus point to the actual site targeted by the specific approach-guided needle.

## Results

Ten right-sided image-enhanced brachial plexus MRNs were obtained. In figure 1, we present the single-frame frontal slab composite MRNs of the brachial plexus for six of those individuals.

The nerve roots, derived from the ventral primary rami that arise at the dorsal root ganglia, are generally well delineated. In a few individuals, even the dorsal primary rami that supply the posterior neck muscles and skin can be seen. To some degree, the subsequent branching structure tends to follow the classic pattern succession of trunks, divisions, cords, and branches, but this is subject to significant individual variation.

Certain bony structures—the coracoid process, medial acromion, clavicle, and humeral head—were colorized and left in place. In these composite frontal view MR neurographs, the subclavian veins are readily evident, with descending pectoral venous branches. In some individuals, the internal and jugular veins are well delineated. The subclavian artery is suppressed because of the use of artifact-suppressive saturation bands.

For coracoid-based approaches, Wilson *et al.*[8] studied 20 male and 20 female patients in the supine position, with arms adducted. With the needle placed initially 2 cm medial and 2 cm caudad to the coracoid process, they advanced the stimulator-directed needle posteriorly to a depth of $4.2 \pm 1.49$ cm (2.25–7.75 cm) in men and $4.01 \pm 1.29$ cm (2.25–6.5 cm) in women, with a 94.8% success rate. The depth in question related to the image-determined posterior distance to the anterior aspect of the axillary artery. In their study measurements, the anterior midpoint of the coracoid process was used as the zero reference point. In this limited study of 10 subjects, we pursued the mediocaudad recommendations of Wilson *et al.* to determine the part of the brachial plexus that would be targeted by a posteriorly directed needle. The targeting error, defined as the ver-

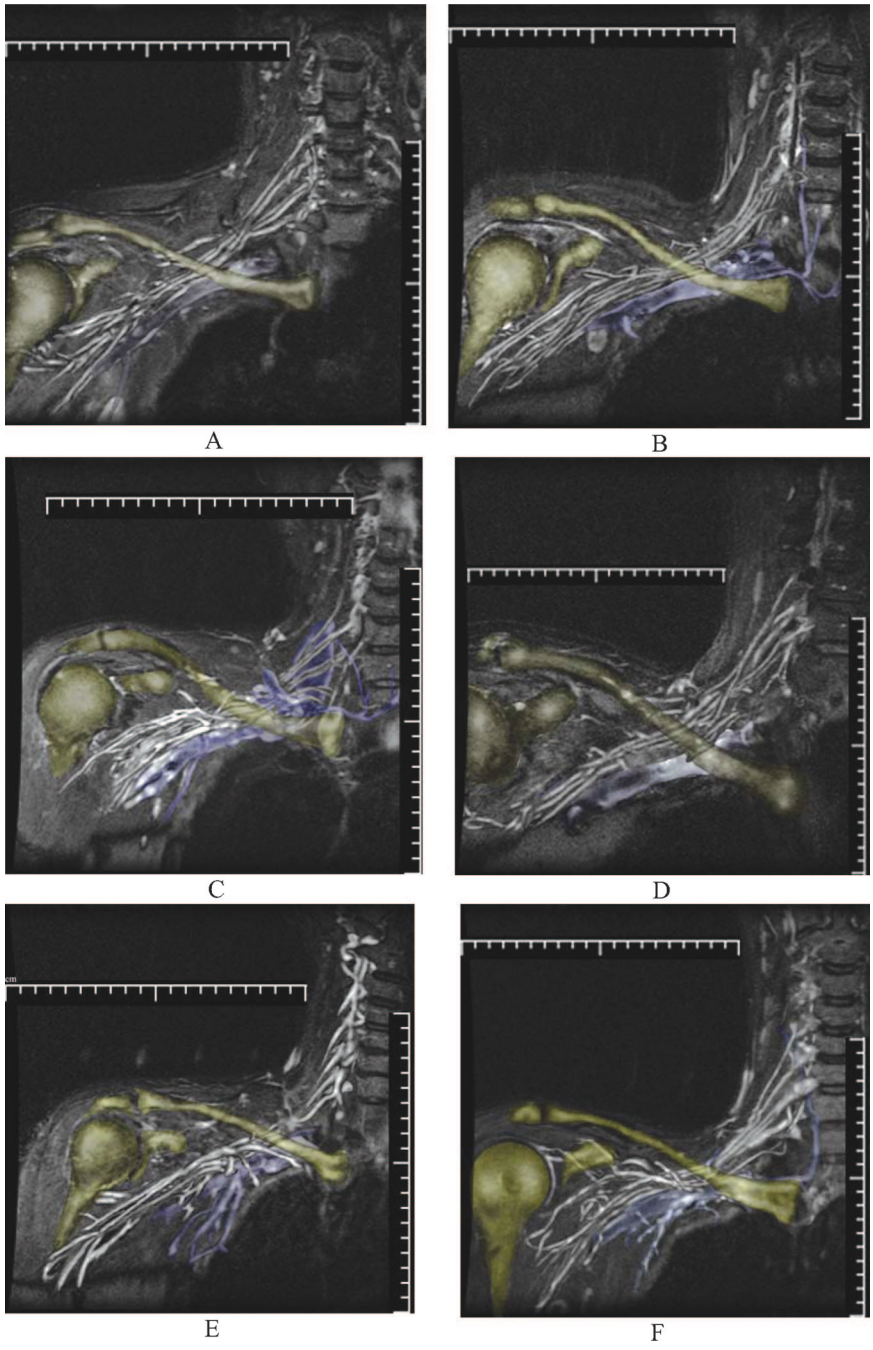


**Fig. 1. Brachial plexus images for six individuals obtained with frontal slab composite magnetic resonance neurography.**

tical distance between the MRN plexus midpoint (*y* in fig. 2) and the Wilson targeted point, was positive if the Wilson approach point was above the MRN midpoint and negative if below it. As a starting point, we used a point on the coracoid process 0.5 cm from its medial edge. In 6 of the 10 subjects, the needle tip led directly toward the midpoint of the brachial plexus. In 2 subjects, the needle tip was directed to the lateral superior edge of the plexus, at a point close to the musculocutaneous nerve takeoff (2 subjects), and in another subject, it was distal to the musculocutaneous nerve takeoff. For these three cases, a recommendation of 2.5–3 cm medial to the coracoid process would have resulted in better positioning. In one subject (fig. 1D), the needle path completely missed the brachial plexus and ended up a full 2 cm above the lateral plexus, 3.4 cm away from the plexus midpoint. This individual was tall and had the longest clavicle (26.5 cm) in the group. Based on these preliminary observations and subject to confirmation by a larger MR study, we conclude that the needle skin placement recommendation of Wilson *et al.* targets well the brachial plexus in average-sized individuals. The average distance of the entry point above the ideal midplexus target was 0.65 ± 0.68 cm (range, −0.76 to 3.38 cm). The recommendation scheme may require, for broad-shouldered individuals, a more medial and more

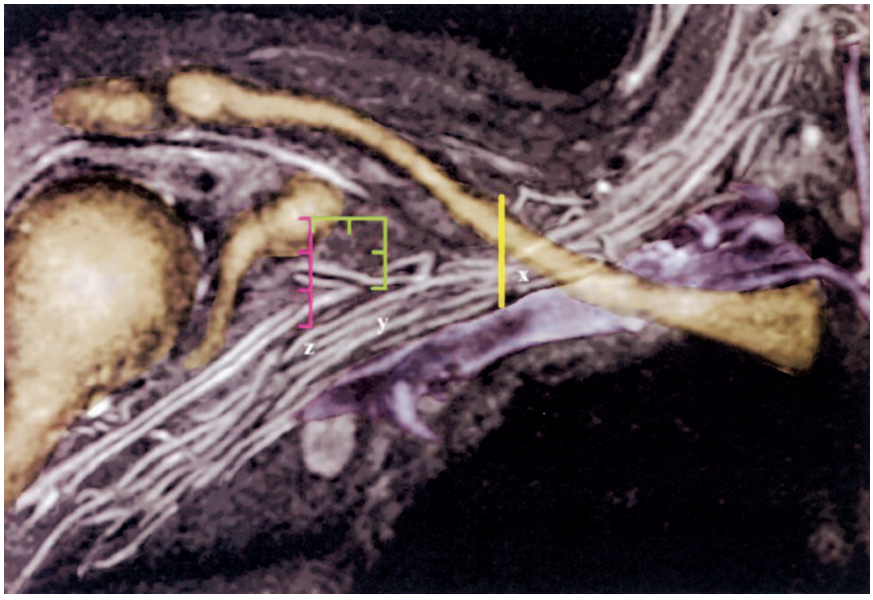


**Fig. 2. A vertical centimeter scale is placed to measure the error associated with each of the three infraclavicular block approaches—midclavicular, mediocaudad to coracoid, and infracoracoid. The approach error was defined as the distance between the plexus midpoint and the actual point on the plexus targeted by a posteriorly directed needle, as recommended by a specific approach. The letters *x*, *y*, and *z* represent the plexus midpoint ideally targeted by the midclavicular, mediocaudad to coracoid, and infracoracoid approaches, respectively. The *yellow stripe* is at the midclavicle.**

caudad skin entry point. In column II of figure 3, we show an illustrative oblique sagittal slice from each of two subjects in our study, which shows the position of the brachial plexus in relation to the coracoid process, as per the Wilson approach.

An infracoracoid process approach was advocated by Kapral *et al.*,[9] namely, that after needle contact with the coracoid process, the needle should be reinserted 2–3 cm immediately caudad to the coracoid process. The targeting error was defined in the same manner as that used with the Wilson approach. In figure 2, *z* denotes the MRN plexus infracoracoid midpoint. Consistent with the more caudad course of the plexus in this region, in 5 of the 10 cases, a 3-cm caudad approach led to a midplexus position, and in 3 cases, a 2.5-cm caudad entry point led to the plexus midpoint. In one individual (D), the 3-cm caudal recommendation targeted the superior edge of the lateral plexus. In the broad-shouldered individual mentioned above, the 3-cm recommendation led to a position 1 cm cephalad to the lateral plexus branches. In summary, the Kapral approach leads to overall results similar to those indicated by Wilson. The targeting error, using the 3-cm caudad approach recommendation, was 0.99 cm ± 1.22 cm (range, −0.34 to 3.84 cm). Column III of figure 3 shows, from two subjects, the representative oblique sagittal cross-sectional view of the coracoid-to-plexus relation in this more lateral region.

In the midclavicle (marked with a yellow vertical bar), the frontal image width of the plexus is at its narrowest (approximately 3 cm in width), which suggests the use

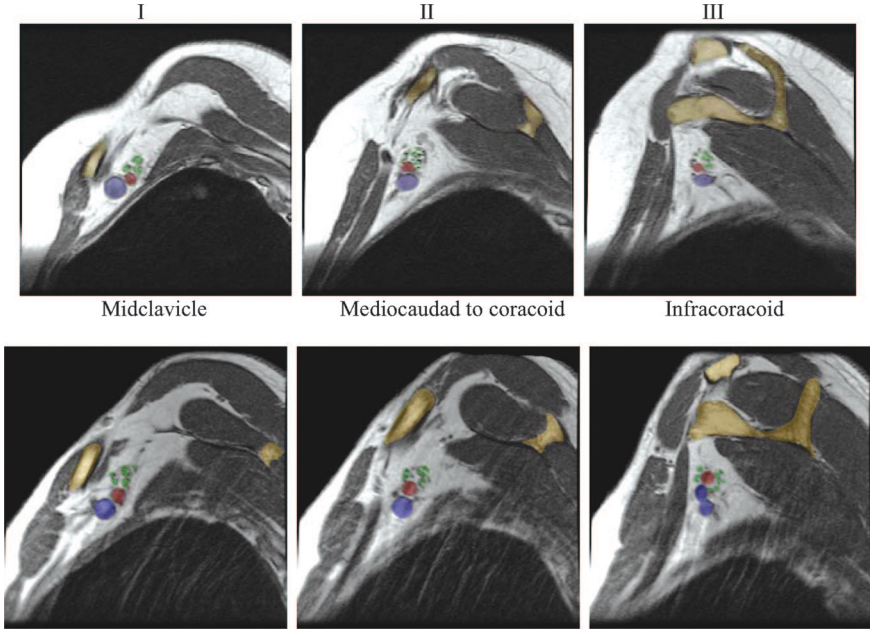


**Fig. 3. For two subjects, the corresponding oblique sagittal views associated with needle placement at the following positions are shown: *column I*, midclavicular; *column II*, 2 cm medial and 2 cm caudal to coracoid; and *column III*, 3 cm infracoracoid.**

**Table 1. Individual Infraclavicular Block Approach Data**

| Patient Code | Age, yr | Sex | Weight, kg | Height, cm | Length of Collarbone, cm | Targeting Error: Wilson Approach (y) | Targeting Error: Kapral Approach (z) | Targeting Error: (AC − SC) Midclavicular Approach (x) | Targeting Error: (VA − JN) Kilka Midclavicular Approach (x) | Angle of the Plexus (Relative to Horizontal) for Midclavicular Approach, ° |
|---|---|---|---|---|---|---|---|---|---|---|
| A | 45 | F | 65.8 | 163.6 | 19.00 | 1.11 | 1.49 | 0.33 | 0.16 | 35.0 |
| B | 58 | F | 77.1 | 162.6 | 19.00 | 1.00 | 0.66 | 0.77 | 0.54 | 21.0 |
| C | 47 | M | 68.9 | 165 | 17.00 | 0.76 | 0.61 | 0.30 | −0.54 | 19.0 |
| D | 59 | M | 86.2 | 182.9 | 26.00 | 3.38 | 3.84 | 1.37 | 0.71 | 32.0 |
| E | 48 | F | 75.3 | 158.8 | 14.75 | −0.39 | −0.34 | 1.20 | 1.44 | 27.0 |
| F | 45 | F | 58.9 | 177.8 | 19.00 | 0.00 | −0.11 | 1.51 | 1.14 | 18.0 |
| G | 27 | F | 63.5 | 165 | 18.00 | 0.63 | 1.83 | −0.31 | −0.51 | 32.0 |
| H | 29 | F | 52 | 157.5 | 15.75 | 0.00 | 0.42 | −0.30 | −0.01 | 30.0 |
| I | 56 | F | 58.9 | 160 | 15.00 | −0.76 | 0.18 | 1.34 | 0.97 | 31.0 |
| J | 44 | M | 81.65 | 182 | 16.50 | 0.82 | 1.37 | 0.44 | 0.34 | 33.0 |
| Mean | 47 | | 68.8 | 167.5 | 18 | 0.65 | 0.99 | 0.67 | 0.43 | 27.8 |
| SD | 10 | | 11 | 9.6 | 3.3 | 1.14 | 1.22 | 0.68 | 0.67 | 6.2 |
| Minimum | 29 | | 52 | 160 | 14.8 | −0.76 | −0.34 | −0.31 | −0.54 | 18.0 |
| Maximum | 59 | | 86.2 | 182.9 | 26 | 3.38 | 3.84 | 1.51 | 1.44 | 35 |

AC = acromioclavicular joint; JN = jugular notch; SC = sternoclavicular joint; VA = ventral acromion.

of the midclavicle as a site suitable for a single injection technique. For infraclavicular blockade, Kilka *et al.*[10] suggested that initial needle placement be made posteriorly just under the midclavicle. Kilka defined the midclavicle as half the distance between the ventral acromion (VA) and the middle of the jugular (suprasternal) notch (JN), *i.e.*, midclavicle = ½(VA − JN). Alternatively, it is possible to define the midclavicle as the midpoint between the acromioclavicular (AC) joint and the sternoclavicular (SC) joint, *i.e.*, as midclavicle = ½(AC − SC). For our 10 subjects, the difference (mean ± SD) between these two methods of determining the midclavicle site is −0.241 ± 0.35 cm. In 8 of 10 subjects, the Kilka acromion-to-jugular notch approach resulted in a midclavicle location slightly more medial than the method based on use of the two ends of the clavicle.

To obtain a targeting error estimate *via* the Kilka method, with use of the ½(VA − JN) calculation, we located the MRN plexus midpoint (*x* in fig. 2) and the corresponding Kilka recommended midpoint and vertically projected these points to the clavicle immediately above; the targeting error was then defined as the distance *along the clavicle* between the Kilka and MRN projections. The targeting error was positive if the MRN clavicle midpoint was medial, *i.e.*, to the right of the Kilka clavicle midpoint, and negative if it was to the left. The targeting results are shown in table 1. In 7 of the 10 cases, this recommendation led to satisfactory needle targeting within the plexus. In 2 subjects, the Kilka target was at the superior edge of the lateral plexus, and in the 1 other subject, it was approximately 0.5 cm cephalad to the lateral trunk. The mean targeting error was 0.43 cm ± 0.67 (range, −0.54 to 1.44). Hence, the Kilka approach is associated with the smallest mean targeting error of the three infraclavicular approaches using a posteriorly directed needle. The results using the ½(AC − SC) midclavicle calculation, as shown in table 1, were comparable.

We calculated the angle (in degrees) in the frontal slab composite coronal plane at which the plexus courses laterally beyond the midclavicle. Relative to a horizontal line drawn through the true midplexus site x, we calculated the angle between points x (midplexus at midclavicle) and z (midplexus at infracoracoid). As shown in table 1, the mean angle is 27.8° ± 6.2° (range, 18°–35°).

In column I of figure 3, we have from two subjects an oblique sagittal cross-section of the brachial plexus at the midclavicle position.

In a study of 10 volunteers, Klaastad *et al.*[11] also noted that the midpoint of the clavicle was lateral to the crossing of the subclavian artery by 17 mm (19–23 mm). Only in one volunteer was the distance less than 10 mm. Hence, Klaastad *et al.* concluded that the clavicular midpoint and the subclavian artery crossing are not clinically interchangeable reference points. Our findings are consistent with this conclusion but indicate a lesser degree of laterality of the clavicular midpoint than the Klaastad study. In table 1, for a needle positioned perpendicular to the skin, our results indicate that the averaged ideal anatomical reference point, so as to achieve localization of the midplexus immediately below the clavicle, is a point approximately 4–5 mm medial to the midclavicle (measured along the clavicle).

In the same study, Klaastad suggested modifications to the infraclavicular block approach of Raj *et al.*,[12] which is essentially a midclavicular approach. As described by Klaastad and Borgeat *et al.*,[13] the modified Raj approach requires that the arm be abducted to 45–90° and elevated to 30°; the needle should be inserted 1 cm below the midclavicle [½(VA − JN)] and angled toward the

emergence of the axillary artery in the fossa axillaris. By comparison in our study, all subjects had the arms adducted. We question whether it is appropriate to make a targeting error comparison with this positional difference, because the effect of arm abduction is to alter the relative locations of key landmarks. Nonetheless, the anatomical findings and recommendations of Klaastad and Borgeat are largely consistent with our own imaging results.

## Discussion

We have developed an approach that we have called the frontal slab composite MRN approach, which exploits the weak selective highlighting of nerves in MR STIR and T1 spin echo sequences. Through the use of a composite of several slices (as opposed to successive visualization of single MR slices) and through the frontal projection of the underlying slices onto a single 2-D slice, an image segmentation of the brachial plexus is achieved in the form of a composite 3-D volume-rendered image, as shown in figure 1, wherein the entirety of the brachial plexus can be seen in an instant.

Representative oblique sagittal cross-sectional views of the plexus for the three infraclavicular block approaches are shown in the two rows of figure 3.

Image-processed frontal slab composite 3-D rendered MRNs of the brachial plexus have educational value in illustrating the significant individual variation, a feature that is difficult to quantify. There are at least 29 documented anatomical variants in the organization or course of brachial plexus components. These variants diverge from the conventional textbook presentation of the plexus interconnections. For example, for the median nerve, the site of union between its branches from the lateral and medial cords is quite variable and has been found as far down as the elbow. Similarly, the musculocutaneous nerve arises from the lateral cord (90.5% of 75 arms), from the lateral and posterior cord (4%), from the median nerve (2%), as two separate bundles from the medial lateral cords (1.4%), or from the posterior cord (1.4%). Instead of piercing the coracobrachialis muscle, the musculocutaneous nerve adheres to the median nerve for some distance down the arm and then passes between the biceps and coracobrachialis muscles (approximately 22% of cases). These and other variations are detailed in the referenced compendium.[14]

The obtained MRNs reproduce the natural skin plane in the region of the plexus that would directly face the anesthesiologist performing the nerve block and allow for the envisioning of the nerve structures beneath the skin in the anesthesiologist's line of sight.

Without access to imaging technology, a clinician must rely on specific palpable anatomical landmarks to achieve needle access to the plexus. In this regard, high-frequency ultrasound[15] has gained momentum as an imaging technology that can image peripheral nerves, but the modality is practically limited to nerves within 2 cm of the skin surface. Coarser quality ultrasound nerve images are obtained at greater depths, such that the degraded echotexture makes them difficult to distinguish from tendons.[16] Ultrasound does not provide an overview of the entirety of the plexus, but rather it generates a focused view of a segment of the brachial plexus.

If it is possible to achieve visualization of the entirety of the brachial plexus, as with an MRN brachial plexus image, one has in principle an infinite number of potential skin entry points to access the brachial plexus with a directed regional block needle. With conventional noninteractive MR imaging devices, access to the patient is still an issue. Nor is quick MR image visualization yet a practical clinical reality owing to greater cost and long scanning times (approximately 30 min in this study) in comparison to ultrasonography, which uses a portable, handheld, and readily activated device. Nonetheless, the MR image postprocessing discussed herein, which is achievable with inexpensive commercial software, clearly enhances the results of presently attainable MR neurographs. The improved MR images are of educational value and demonstrate the considerable individual variation. Whether this image postprocessing enhancement procedure can be programmed for possible automated use in an interactive MR suite requires further investigation.

## References

1. Filler AG, Hayes CE, Kliot M, Winn HR, Bell BA, Tsuruda JS: Magnetic resonance neurography. Lancet 1993; 341:659–61
2. Filler AG, Kliot M: Application of magnetic resonance neurography in the evaluation of patients with peripheral nerve pathology. J Neurosurg 1996; 85:299–309
3. Maravilla KR, Bowen BC: Imaging of the peripheral nervous system: Evaluation of peripheral neuropathy and plexopathy. Am J Neuroradiol 1998; 19:1011–23
4. Elster AD, Burdette JH: Questions and Answers in Magnetic Resonance Imaging, 2nd edition. St. Louis, Mosby, pp 239–40
5. De Verdier HJ, Colletti PM, Terk MR: MRI of the brachial plexus: A review of 51 cases. Computerized Imaging and Graphics 1993; 17:45–50
6. Posniak HV, Olson MC, Dudiak CM, Wisniewski R, O'Malley C: MR imaging of the brachial plexus. Am J Roent 1993; 161:373–9
7. Van Es HW, Den Berg V, Franssen H, Witkamp TD, Ramos L, Feldberg MAM, Wokke JHJ: Magnetic resonance imaging of the brachial plexus in patients with multifocal motor neuropathy. Neurology 1997; 48:1218–24
8. Wilson JL, Brown DL, Wong GY, Ehman RL, Cahill DR: Infraclavicular brachial plexus block: parasagittal anatomy important to the coracoid technique. Anesth Analg 1998; 87:870–3
9. Kapral S, Jandrasits O, Schabernig C, Likar R, Reddy B, Mayer N, Weinstabl C: Lateral infraclavicular plexus block vs. axillary block for hand and forearm surgery. Acta Anesthesiol Scand 1999; 43:1047–52
10. Kilka HG, Geiger P, Mehrkens HH: Infraclavicular vertical brachial plexus blockade: A new technique of regional anaesthesia. Anaesthetist 1995; 44:339–44
11. Klaastad O, Lilleas FG, Rotnes JS, Breivik H, Fosse E: A magnetic resonance imaging study of modifications to the infraclavicular brachial plexus block. Anesth Analg 2000; 91:929–33
12. Raj PP, Montgomery SJ, Nettles D, Jenkins MT: Infraclavicular brachial plexus block: A new approach. Anesth Analg 1973; 52:897–903
13. Borgeat A, Ekatodramis G, Dumont C: An evaluation of the infraclavicular block via a modified approach of the Raj technique. Anesth Analg 2001; 93:436–41
14. Bergman RA, Thompson SA, Akifi AK, Saadeh FA: Compendium of Human Anatomic Variation. Baltimore, Urban and Schwarzenberg, 1988, pp 138–43, 474–84
15. Retzl G, Kapral S, Greher M, Mauritz M: Ultrasonographic findings of the axillary part of the brachial plexus. Anesth Analg 2001; 92:1271–5
16. Silvestri E, Martinoli C, Derchi LE, Bertolotto M, Chiaramondia M, Rosenberg I: Echotexture of peripheral nerves: Correlation between US and histologic findings to differentiate tendons. Radiology 1995; 197:291–6